Non-Gaussian noise without memory in active matter

Étienne Fodor,[1,2,3] Hisao Hayakawa,[3] Julien Tailleur,[2] and Frédéric van Wijland[2,3]
[1]DAMTP, Centre for Mathematical Sciences, University of Cambridge, Wilberforce Road, Cambridge CB3 0WA, United Kingdom
[2]Laboratoire Matière et Systèmes Complexes, UMR No. 7057, CNRS/P7, Université Paris Diderot, 10 Rue Alice Domon et Léonie Duquet, 75205 Paris, Cedex 13, France
[3]Yukawa Institute for Theoretical Physics, Kyoto University, Kitashirakawa-oiwake cho, Sakyo-ku, Kyoto 606-8502, Japan

(Received 27 September 2018; published 17 December 2018)

Modeling the dynamics of an individual active particle invariably involves an isotropic noisy self-propulsion component, in the form of run-and-tumble motion or variations around it. This nonequilibrium source of noise is neither white—there is persistence—nor Gaussian. While emerging collective behavior in active matter has hitherto been attributed to the persistent ingredient, we focus on the non-Gaussian ingredient of self-propulsion. We show that by itself, that is, without invoking any memory effect, it is able to generate particle accumulation close to boundaries and effective attraction between otherwise repulsive particles, a mechanism which generically leads to motility-induced phase separation in active matter.

DOI: 10.1103/PhysRevE.98.062610

I. INTRODUCTION

The Brownian dynamics of particles interacting via conservative forces inevitably leads, whatever the level of friction, to a steady-state distribution given by the celebrated Gibbs-Boltzmann distribution. The key property allowing this statement to be made without having to solve for the dynamics is detailed balance, a signature of time reversibility. Granted, whatever the specifics of time reversal, it is synonymous with equilibrium behavior and it comes closely associated with a number of well-known consequences, such as the fluctuation-dissipation theorem [1] or a vanishing entropy production. In active matter, by contrast, the interest is in particles whose individual motion, while isotropic, relies on a net dissipation of energy. Such systems leave the realm of equilibrium physics, and the the possibility exists for a wealth of phenomena that our equilibrium intuition often fails to grasp [2–11].

Focusing on the subclass of active systems made of isotropic particles, a variety of microscopic dynamics have been proposed to model individual motion. Run-and-tumble particles (RTPs), for which directed motion is interspersed with random directional changes, are among the most studied of models and have been used to model swimming bacteria [12,13]. Active Brownian particles (ABPs), in which a Gaussian white noise drives directional diffusion at an otherwise constant tangential velocity, provide a simple model for self-propelled colloids [5,11,14–18]. In such models, instead of a standard equilibrium Gaussian white noise mimicking the action of the solvent on the particles, one has to deal with a random force that is neither Gaussian nor white.

In an effort to further simplify such active particle models, without however giving up the gist of nonequilibrium activity, it has been argued that the main nonequilibrium ingredient is the existence of some memory, also termed persistence, in the random self-propulsion force. This has led, for instance, to a series of works on active Ornstein-Uhlenbeck particles (AOUPs) [19–25], in which a Gaussian noise characterized by an exponentially decaying memory kernel is used. (See also [26] for a kinetic Monte Carlo version of AOUPs.) In the latter case, of course, no matching memory kernel in the viscous damping is introduced; otherwise one would revert to equilibrium physics as described by Kubo [27] in his works on generalized Langevin equations.[1] Active Ornstein-Uhlenbeck particles have been used, for instance, to model the dynamics of tracers in living systems [29–31].

Our purpose in this work is to investigate what physical characteristics the non-Gaussian nature of the active fluctuations contributes. We will thus take the opposite stance and forget about any type of memory, thereby working with a non-Gaussian but white noise in our equations of motion for the individual particles. In practice, we consider particles experiencing a viscous drag, a random force, and either external or interparticle forces:

$$m\frac{d\mathbf{v}_i}{dt} = -\gamma\mathbf{v}_i + \mathbf{F}_i + \gamma\boldsymbol{\eta}_i. \tag{1}$$

Here m is the mass of the particles, which we send to zero to describe an overdamped limit, but keep finite in our simulations for practical purposes explained below. We consider a non-Gaussian white noise $\boldsymbol{\eta}$, known as a filtered Poisson process with a Dirac kernel: Over a given time interval of duration $t_{\rm obs}$, a number n of times $\{t_1, \ldots, t_n\}$ is drawn at random from a Poisson distribution with average $\nu t_{\rm obs}$. These times are themselves random variables drawn from a uniform distribution over $[0, t_{\rm obs}]$. At each time t_i a random vector $\boldsymbol{\ell}_i$ is independently drawn from some specified jump distribution

[1]Unless, of course, there is some imbalance between force correlations and viscous damping characterized by different memory kernels [28].

$p(\boldsymbol{\ell})$ so that

$$\boldsymbol{\eta}(t) = \sum_{i=1}^{n} \boldsymbol{\ell}_i \delta(t - t_i). \quad (2)$$

Interestingly, our main message is that such non-Gaussian dynamics exhibits much of the standard active matter behaviors frequently associated with persistent noises, such as accumulation close to boundaries.

Langevin equations driven by a non-Gaussian white noise have been considered before. An early instance can be found in signal processing [32], but other developments have been witnessed in mechanical and structural engineering [33–38], including processes involving multiplicative noise, or even more recently in finance [39,40]. From a physics perspective, some properties of the harmonic oscillator evolving under a non-Gaussian white noise have been solved exactly [41,42]. More complex force fields or noises have been investigated earlier [37,43,44]. More recently, it was shown how to properly formulate the ideas of stochastic thermodynamics in the presence of non-Gaussian white noise [45] and actual physical realizations have been brought forth [46–49]. These few references do not by any means make up an exhaustive review. An important feature that is absent from all these works, however, is that no collective effects (between various particles evolving with such modified Langevin dynamics) are considered.

Before we consider interacting particle systems, we first discuss in Sec. II the properties of the microscopic dynamics that we endow our particles with. The specifics of a non-Gaussian but white noise are described there. We focus, analytically and numerically, on a single particle evolving in an external potential, considering in particular a particle confined in a harmonic trap and a particle in the vicinity of a wall. This study of one-body problems is designed to lay the foundation for the many-particle case that we consider in Sec. III. We first establish that, as for persistent active particles, quorum-sensing interactions that make motility decrease at high density lead to a motility-induced phase separation (MIPS) [3,7,50]. Simulations of large bidimensional systems of non-Gaussian particles interacting via pairwise forces are numerically beyond what we can achieve and we thus could not establish MIPS in this case [5,16,51]. We nevertheless show that, as for ABPs, RTPs, or AOUPs, purely repulsive forces induce an effective attraction between the particles. To interpret what we observe, we describe the dynamics of collective modes and we build an evolution equation for the local particle density à la Dean and Kawasaki [52,53]. We use that equation to construct the Bogoliubov-Born-Green-Kirkwood-Yvon (BBGKY) hierarchy of correlations [54] and we derive a low-density expansion of correlation functions.

II. SINGLE-PARTICLE DYNAMICS

A. Modified Langevin dynamics

In order to pose our problem with care, we begin with the single-particle version of the dynamics (1)

$$m\frac{d\mathbf{v}}{dt} = -\gamma\mathbf{v} + \mathbf{F} + \gamma\boldsymbol{\eta}, \quad (3)$$

where $\mathbf{F} = -\partial_{\mathbf{r}} U$ is taken to be a conservative force deriving from the potential U. The factor γ in front of $\boldsymbol{\eta}$ is here for practical reasons, as we prefer thinking of the noise $\boldsymbol{\eta}$ as a fluctuating velocity imparted to the particle.

Exploiting the definition of the non-Gaussian noise $\boldsymbol{\eta}$ in Eq. (2), the generic average brackets $\langle\cdot\rangle$, referring to an average over the noise realizations, thus denote an average with respect to n, to the t_i's, and to the $\boldsymbol{\ell}_i$'s. The generating functional of $\boldsymbol{\eta}$ is

$$Z[\mathbf{h}] = \left\langle \exp\left(\int dt\, \mathbf{h}\cdot\boldsymbol{\eta}\right)\right\rangle = \exp\left[\nu \int dt (\langle e^{\boldsymbol{\ell}\cdot\mathbf{h}(t)}\rangle_p - 1)\right], \quad (4)$$

where $\langle\cdot\rangle_p$ denotes an average with respect to $p(\boldsymbol{\ell})$ only. A key property is that the nth-order cumulant of $\boldsymbol{\eta}$ is nonzero only when the arguments are at equal times,

$$\langle \eta^{\alpha_1}(t_1)\cdots\eta^{\alpha_n}(t_n)\rangle_c = \kappa^{(n)}_{\alpha_1,\ldots,\alpha_n}\delta(t_1 - t_2)\cdots\delta(t_{n-1} - t_n), \quad (5)$$

where $\kappa^{(n)}_{\alpha_1,\ldots,\alpha_n} = \nu\langle \ell^{\alpha_1}\cdots\ell^{\alpha_n}\rangle_p$. The α_j's denote arbitrary space directions $\alpha_i = 1,\ldots,d$, where d is the number of spatial dimensions. In the following, we consider that only the even cumulants of the noise are nonzero.

The celebrated Gaussian white noise is recovered in the scaling limit $\nu \to \infty$ and $\langle \ell^\alpha \ell^\beta\rangle_p \to 0$, with the effective diffusion constant $\gamma^{-1}T = (2d)^{-1}\nu\langle\boldsymbol{\ell}^2\rangle_p$ being fixed. In the latter scaling limit, the dynamics is equilibrium and, for instance, the fluctuation-dissipation theorem follows. For the purpose of comparison to equilibrium, we will stick to the notation $T = \gamma(2d)^{-1}\nu\langle\boldsymbol{\ell}^2\rangle_p$ even if out of equilibrium. One must keep in mind that T then loses its thermodynamic meaning of a temperature. However, a curiosity of Eq. (3) is that it nevertheless preserves some sort of an equipartition theorem, according to which $\langle m\mathbf{v}^2/2\rangle = dT/2$ and $\langle \mathbf{r}\cdot\partial_{\mathbf{r}} U\rangle = dT$.

Just as its Gaussian counterpart, Eq. (3) can also be considered in the overdamped limit. In that limit, somewhat unphysical features emerge that only $m \neq 0$ helps regularize. Considering the overdamped version

$$\gamma\mathbf{v} = \mathbf{F} + \gamma\boldsymbol{\eta}, \quad (6)$$

one can see that after a given pulse the dynamics is the deterministic gradient descent. Then, after a typical time ν^{-1}, an instantaneous pulse occurs again, with an infinite amplitude. For finite forces $\mathbf{F}$, the infinite amplitude will always win over, and this leads to the particle jumping instantaneously from one place to another, possibly flying over existing obstacles. In practice, this makes simulations particularly difficult in that limit. In the Gaussian limit, such events become rarer due to the vanishing of the hopping amplitude, but it is a well-known fact that the Brownian trajectory is nondifferentiable and that sampling a Gaussian white noise too can induce, however rarely, unphysical displacements. We will return to these caveats when considering interacting particles in Sec. III.

Using the Kramers-Moyal expansion, the master equation for the probability $P(\mathbf{x},t)$ that the particle lies at $\mathbf{r}(t) = \mathbf{x}$ reads

$$\partial_t P = \gamma^{-1}\partial_{\mathbf{x}}\cdot(\mathbf{F}P) + \partial_{\alpha_1} D_{\alpha_1} P, \quad (7)$$

where we have used the notation

$$D_{\alpha_1} = \sum_{n\geqslant 2} \frac{(-1)^n \kappa^{(n)}_{\alpha_1,\ldots,\alpha_n}}{n!} \frac{\partial^{n-1}}{\partial x_{\alpha_2}\cdots\partial x_{\alpha_n}}, \tag{8}$$

which generalizes the diffusive gradient $\gamma^{-1}T\partial_{\mathbf{x}}$ [55–57]. A somewhat more formal way of defining this operator is

$$\mathbf{D}_{\mathbf{x}} = \nu\frac{\tilde{p}(i\partial_{\mathbf{x}})-1}{i\partial_{\mathbf{x}}}, \tag{9}$$

where $\tilde{p}(\mathbf{k}) = \int_{\boldsymbol{\ell}} e^{-i\mathbf{k}\cdot\boldsymbol{\ell}} p(\boldsymbol{\ell})$. The last term in (7) also stems from the more intuitive master equation balance

$$\partial_{\alpha_1} D_{\alpha_1} P = \nu\int_{\boldsymbol{\ell}} p(\boldsymbol{\ell})[P(\mathbf{x}-\boldsymbol{\ell},t) - P(\mathbf{x},t)]. \tag{10}$$

In what follows, we consider that $\boldsymbol{\eta}$ is a symmetric process where the jump distribution is isotropic.

B. Specific jump distributions

For the sake of clarity, we consider a specific jump distribution given by

$$p(\boldsymbol{\ell}) = \mathcal{N}_{d\alpha}(\ell/a)^{\alpha-1}e^{-\ell/a}, \tag{11}$$

where $d+\alpha > 1$ and $\ell = |\boldsymbol{\ell}|$. The normalization constant reads

$$\mathcal{N}_{d\alpha} = [\Omega_d a^d \Gamma(\alpha+d-1)]^{-1}. \tag{12}$$

The solid angle in d dimension $\Omega_d = 2\pi^{d/2}/\Gamma(d/2)$ is written here in terms of the Euler Gamma function Γ. Such distributions typically emerge when considering that the jump length is the sum of α Poisson processes. We recover an exponential distribution for $\alpha = 1$, and the distribution gets all the more peaked around its average value as α increases. For such a distribution $\langle\boldsymbol{\ell}^2\rangle_p = a^2(d+\alpha)(d+\alpha-1)$, so the diffusion constant $D = \gamma^{-1}T = \nu\langle\boldsymbol{\ell}^2\rangle_p/2d$ is of order νa^2.

To obtain the corresponding form of the operator $\mathbf{D}_{\mathbf{x}}$ in Eq. (9), we use the following expressions of the spatial Fourier transforms for the isotropic distributions (11):

$$\begin{aligned}
\tilde{p}(q) &= \int_{-\infty}^{\infty} e^{iq\ell}p(\ell)d\ell \\
&= \frac{(1-iaq)^\alpha + (1+iaq)^\alpha}{2[1+(aq)^2]^\alpha} \quad \text{for } d=1,\\
\tilde{p}(q) &= 2\pi\int_0^\infty \ell J_0(q\ell)p(\ell)d\ell \\
&= {}_2F_1\left[\frac{1+\alpha}{2},\frac{2+\alpha}{2};1;-(aq)^2\right] \quad \text{for } d=2,\\
\tilde{p}(q) &= 4\pi\int_0^\infty \frac{\ell}{q}\sin(q\ell)p(\ell)d\ell \\
&= \frac{\sin[(1+\alpha)\arctan(aq)]}{aq(1+\alpha)[1+(aq)^2]^{(1+\alpha)/2}} \quad \text{for } d=3,
\end{aligned} \tag{13}$$

where J_0 and ${}_2F_1$ denote the Bessel function of the first kind and the Gauss hypergeometric function, respectively. We report in Table I the explicit form of $\mathbf{D}_{\mathbf{x}}$ for some specific values of d and α.

TABLE I. Explicit form of the operator $\partial_{\mathbf{x}}\cdot\mathbf{D}_{\mathbf{x}}/\nu a^2$ in (9), expressed in terms of $L_0 = 1 - a^2\partial_{\mathbf{x}}^2$ for the jump distribution (11). We consider some specific values of the spatial dimension d and of the jump parameter α.

$\frac{\partial_{\mathbf{x}}\cdot\mathbf{D}_{\mathbf{x}}}{\nu a^2}$	$d=1$	$d=2$	$d=3$
$\alpha=0$		$\frac{L_0^{-1/2}-1}{a^2}$	$\frac{\partial_{\mathbf{x}}^2}{L_0}$
$\alpha=1$	$\frac{\partial_{\mathbf{x}}^2}{L_0}$	$\frac{1}{a^2}(L_0^{-3/2}-1)$	$\frac{L_0+1}{L_0^2}\partial_{\mathbf{x}}^2$
$\alpha=2$	$\frac{2+L_0}{L_0^2}\partial_{\mathbf{x}}^2$	$\frac{1}{a^2}\left(\frac{3-L_0}{2L_0^{5/2}}-1\right)$	$\frac{3L_0(L_0+1)+4}{3L_0^3}\partial_{\mathbf{x}}^2$

C. Harmonic trap

It is a well-documented fact, as reviewed by Solon *et al.* [58], that for both RTPs and ABPs evolving in a quadratic potential, there can be an overshoot of the probability to find the particle at a finite distance from the center of the trap. An active particle with a finite propulsive force $\mathbf{F}_{\mathbf{p}}$ indeed has a horizon $r_{\mathrm{h}} = |\mathbf{F}_{\mathbf{p}}|/k$ for a trapping force $\mathbf{F}_{\mathrm{trap}}(\mathbf{r}) = -k\mathbf{r}$. When the time taken by the particle to cross the trap is much shorter than the persistence time of the propulsive force, the particle spends most of its time at the horizon. The density profile in such cases is not that of a simple decay from a peak at the center of the potential well, but it is actually peaked at $\mathbf{r} \simeq r_{\mathrm{h}}$. Interestingly, this is not observed in AOUPs where the stationary distribution remains a Gaussian [59] (an equilibrium one at that [22]). Thus, a natural question is whether non-Gaussian white noise alone is responsible for a nonmonotonic density profile at odds with the intuition gained from equilibrium. The answer is no, but there are some shared features. For non-Gaussian but white noise, similar calculations have been done in the past, but these do not really apply to the modeling of active particles. For the example worked out in [42], a Lévy-type distribution with exponent α is obtained for the position probability distribution function (PDF) of a particle in one space dimension. This holds for a non-Gaussian white noise that is a symmetric α-stable Lévy process, which is rather far from the sort of non-Gaussian noise that is relevant to active particles. In the latter, a typical hopping scale a exists, as for instance in the jump distributions discussed in Sec. II B. For such jump distributions, it is actually possible to find the Fourier transform of the position PDF of a particle in a harmonic well $V(\mathbf{r}) = k\mathbf{r}^2/2$ with stiffness k. The results are summarized in Table II. They show the Fourier transform of the steady-state distribution $P_{\mathrm{ss}}(\mathbf{r})$, defined by

$$\tilde{P}_{\mathrm{ss}}(\mathbf{q}) = \lim_{t\to\infty}\langle e^{i\mathbf{q}\cdot\mathbf{r}(t)}\rangle. \tag{14}$$

Introducing the response function $\chi(t) = \Theta(t)e^{-t/\tau_r}$, with $\tau_r = \gamma/k$, we may rewrite the Langevin equation (6) for $\mathbf{F} = -k\mathbf{r}$ as

$$\mathbf{r}(t) = \int_{-\infty}^{t}\chi(t-u)\boldsymbol{\eta}(u)du. \tag{15}$$

Therefore, using a cumulant expansion in Eq. (14), we arrive at

$$\ln \tilde{P}_{\rm ss}(\mathbf{q}) = \lim_{t\to\infty}\sum_{n=1}^{\infty}\frac{i^n}{n!}q_{\alpha_1}\cdots q_{\alpha_n} \times \int_{-\infty}^{t}\langle \eta_{\alpha_1}(t_1)\cdots\eta_{\alpha_n}(t_n)\rangle_c \times \chi(t-t_1)\cdots\chi(t-t_n)dt_1\cdots dt_n, \quad (16)$$

where the α_i indices are summed over and run from 1 to d. Substituting the expression for the noise cumulants (5) into Eq. (16), we obtain

$$\ln \tilde{P}_{\rm ss}(\mathbf{q}) = \nu\int_0^{\infty} du(\tilde{p}(\mathbf{q}\chi(u)) - 1). \quad (17)$$

Finally, using the change of variable $u \to s = \chi(u)$, the steady profile can be expressed as

$$\ln \tilde{P}_{\rm ss}(\mathbf{q}) = \nu\tau_r\int_0^{1}\frac{ds}{s}(\tilde{p}(\mathbf{q}s) - 1). \quad (18)$$

One could directly check that Eq. (18) is indeed a solution of Eq. (7) for $\mathbf{F} = -k\mathbf{r}$. We report in Table II explicit analytic expressions for some specific values of α and d. In $d = 2$, the steady-state distribution can always be explicitly computed as

$$\ln \tilde{P}_{\rm ss}(\mathbf{q}) = -\frac{\nu\tau_r(1+\alpha)(2+\alpha)(aq)^2}{8} \times {}_4F_3\left[1, 1, \frac{3+\alpha}{2}, \frac{4+\alpha}{2}; 2, 2, 2; -(aq)^2\right]. \quad (19)$$

The corresponding distributions in real space show interesting features like exponential tails (see [60] for a more mathematical discussion). The discussion depends on the value of the $\nu\tau_r$ combination, whose physical meaning is clear: The higher this number is the more frequently the white noise has stricken during the typical relaxation times within the well.

When the relaxation within the well does not have time to proceed, for $\nu\tau_r \lesssim 1$, the center of the well becomes underpopulated with respect to a Gaussian and the distribution actually becomes convex at the origin where it develops a cusp along with fat tails. For instance, for $\alpha = 1$, in one space dimension, an explicit form of $P_{\rm ss}$ can be found,

$$P_{\rm ss}(x) \sim \left(\frac{|x|}{a}\right)^{(\nu\tau_r-1)/2} K_{(\nu\tau_r-1)/2}\left(\frac{|x|}{a}\right), \quad (20)$$

where K_n is the modified Bessel function of the second kind. A cusp does develop at the origin when $\nu\tau_r < 2$. This regime mirrors that in which RTPs or ABPs exhibit a probability overshoot away from the center of the well; small ν means large persistence time. A non-Gaussian white noise alone, however, is not sufficient to produce an overshoot of the position PDF a finite distance away from the bottom of the harmonic well for the choices of $p(\ell)$ that we have tested. This is probably due to the absence of any mechanism to select a specific length scale in our non-Gaussian models, as opposed to ABPs and RTPs where the depletion of the center of the well leads to an accumulation at the horizon $r_{\rm h}$. Here the depletion instead leads to fat tails.

TABLE II. Space Fourier transform of the steady density profile in Eq. (18) for a α-Γ jump distribution in Eq. (11). We take specific values of the spatial dimension d and the parameter α.

$\tilde{P}_{\rm ss}$	$d = 1$	$d = 3$
$\alpha = 0$		$\frac{1}{[1+(qa)^2]^{\nu\tau_r/2}}$
$\alpha = 1$	$\frac{1}{[1+(qa)^2]^{\nu\tau_r/2}}$	$\frac{\exp\left(-\frac{\nu\tau_r}{2}\frac{(qa)^2}{1+(qa)^2}\right)}{[1+(qa)^2]^{\nu\tau_r/2}}$
$\alpha = 2$	$\frac{\exp\left(-\nu\tau_r\frac{(qa)^2}{1+(qa)^2}\right)}{[1+(qa)^2]^{\nu\tau_r/2}}$	$\frac{\exp\left(-\frac{\nu\tau_r}{6}\frac{(qa)^2[7+5(qa)^2]}{[1+(qa)^2]^2}\right)}{[1+(qa)^2]^{\nu\tau_r/2}}$

In the opposite regime of small a at fixed $\nu\tau_r a^2$, and hence $\nu\tau_r \gg 1$, one recovers the Gaussian behavior $\tilde{P}_{\rm SS}(\mathbf{q}) = e^{-Tq^2/(2k)}$. This regime mirrors ABPs and RTPs which also behave as equilibrium particles in the limit of vanishing persistence [58]. Finally, note that, irrespective of the specific jump distribution $p(\boldsymbol{\ell})$, equipartition holds in the sense that $k\langle \mathbf{r}^2\rangle/2 = dT/2$ in d space dimensions.

D. Accumulation at boundaries

With a view to gaining further intuition on the effect of a non-Gaussian white noise, we continue our exploratory investigations by considering an independent particle interacting with a fixed obstacle. The obstacle is modeled by an external repulsive potential with range σ and energy scale ε, of the form $U(\mathbf{r}) = v(|\mathbf{r}|)\Theta(\sigma - |\mathbf{r}|)$. The potential v is either harmonic $v(r) = \varepsilon(1 - r/\sigma)^2$ or exponential $v(r) = \varepsilon\exp\{-1/[(\sigma/r)^2 - 1]\}$. We restore a nonzero mass for numerical purposes, as discussed in Sec. II A. To probe the overdamped regime, we focus on small values of the inertial time m/γ compared with the obstacle relaxation time $\tau = \gamma\sigma^2/\varepsilon$: The distribution indeed converges to a fixed profile, as shown in Fig. 1.

We measure the evolution of the radial distribution of the particle position away from the obstacle center. The obstacle is located at the center of a two-dimensional (2D) box with periodic boundary conditions. For different values of $\nu\tau$, we compare the profile for non-Gaussian white noise, with jump distribution $p(\boldsymbol{\ell}) \sim e^{-\ell/a}$, and the one for AOUPs with persistence time $1/\nu$. The accumulation at the obstacle boundary $r = \sigma$, shown in Figs. 2(a) and 2(b) for a non-Gaussian white noise, is qualitatively analogous to that found with a persistent noise, reported in Figs. 2(c) and 2(d): It is more and more peaked as $\nu\tau$ decreases. This is consistent with previous results for persistent active particles [21,61–63]. For a harmonic obstacle, the distribution is singular at $r = \sigma$ for non-Gaussian noise, at variance with the persistent case, and a cusp appears for $\nu\tau < 5$, reminiscent of the profile under harmonic confinement. When increasing a/σ at fixed $\nu\tau$, which amounts to increasing the temperature $T \sim \nu a^2$ as shown in in Figs. 2(e) and 2(f), the particle probes deeper regions of the potential, as expected.

Overall, our results support that the particle is effectively attracted to the obstacle boundary for small $\nu\tau$. In this regime, the particle has ample time to go down the potential wall

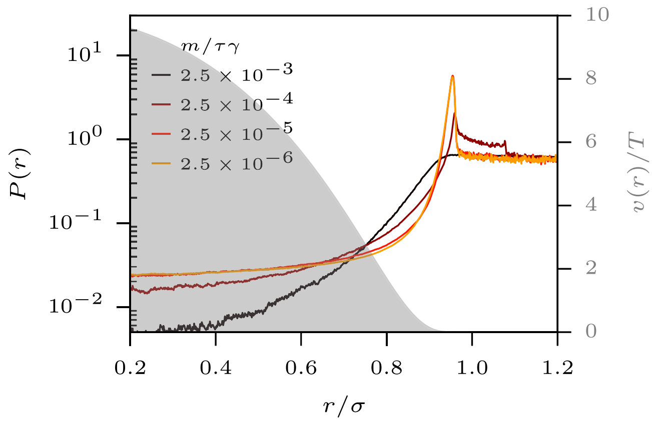

FIG. 1. Numerical results of the distribution of position for a particle subjected to a non-Gaussian white noise in two dimensions. The shaded region represents the form of the potential. The noise has a jump distribution $p(\boldsymbol{\ell}) \sim e^{-\ell/a}$ and the particle evolves in the potential $v(r) = \varepsilon \exp\{-1/[(\sigma/r)^2 - 1]\}\Theta(\sigma - r)$. The position PDF is reported as a function of the distance from the center of the potential for different values of $m/\tau\gamma$, where $\tau = \gamma\sigma^2/\varepsilon$: It converges at small values of $m/\tau\gamma$. The parameters are $T = 1$, $\gamma = 1$, $\varepsilon = 10$, $\sigma = 1$, and $\nu = 20$.

by steepest descent between two successive pulses, with typical time $\tau = \gamma\sigma^2/\varepsilon$. Hence it effectively accumulates down the potential instead of exploring the whole available space uniformly. In short, if the particle ever goes up the wall, it immediately goes down and hence the probability increases right at the edge of the obstacle. Assuming the obstacle can be viewed as a fixed particle, this suggests that effective two-body attraction could emerge in an assembly of particles driven by a non-Gaussian white noise, even though bare interactions are repulsive. A related question is whether these attractive effects, if present, are sufficiently strong to induce MIPS.

III. COLLECTIVE DYNAMICS

A. Quorum sensing interactions

To address interactions between particles, we first consider the case where the statistics of self-propulsion depend on the local density. Such quorum-sensing interactions are relevant to model cells that adapt their motility to their local environments [64], leading to rich collective behaviors [65]. For persistent self-propelled particles, a propulsion speed decreasing as the local density increases has been shown to lead to MIPS [3,50,66]. Furthermore, quorum-sensing interactions can be seen as an effective description of the kinetic slowing down induced by repulsive pairwise forces between particles [50,66–69], despite some important qualitative differences between these models [70,71].

In the context of a non-Gaussian white noise, we model the dynamics of an individual particle by

$$\gamma \frac{d\mathbf{x}_i}{dt} = \boldsymbol{\eta}_i, \tag{21}$$

with the important difference that, now, the noise cumulants $\kappa^{(n)}_{\alpha_1,\ldots,\alpha_n}$ in Eq. (5) depend on the local density $\rho(\mathbf{x},t) = \sum_i \delta^{(d)}(\mathbf{x} - \mathbf{x}_i(t))$:

$$\kappa^{(n)}_{\alpha_1,\ldots,\alpha_n}(\rho) = \nu \int \ell^{\alpha_1} \cdots \ell^{\alpha_n} p_\rho(\boldsymbol{\ell}) d\boldsymbol{\ell}. \tag{22}$$

In practice, this is implemented by assuming that the jump distribution $p_\rho(\boldsymbol{\ell})$ itself is affected by ρ. In addition, each individual noise $\boldsymbol{\eta}_i$ remains independent between particles. The corresponding dynamics for the average density $\hat{\rho}(\mathbf{x},t) = \langle \rho(\mathbf{x},t)\rangle$ reads

$$\partial_t \hat{\rho} = \sum_{n\geqslant 1} \frac{(-1)^n}{n!} \partial_{x_{\alpha_1}} \cdots \partial_{x_{\alpha_n}} \left[\hat{\rho}\kappa^{(n)}_{\alpha_1,\ldots,\alpha_n}(\hat{\rho})\right], \tag{23}$$

which can also be written as

$$\partial_t \hat{\rho} = \nu \int \sum_{n\geqslant 1} \frac{(-\boldsymbol{\ell}\cdot\partial_{\mathbf{x}})^n}{n!} [p_\rho(\boldsymbol{\ell})\hat{\rho}] d\boldsymbol{\ell}. \tag{24}$$

The emergence of a motility-induced phase separation at large scale can then be determined from a linear stability analysis, in the spirit of [50,58].

To do so, we consider fluctuations around the homogeneous profile ρ_0 and work to linear order in $\delta\rho = \hat{\rho} - \rho_0$,

$$\partial_t \delta\rho = \nu \int d\boldsymbol{\ell}[p_\rho(\boldsymbol{\ell}) + \rho_0 p'_\rho(\boldsymbol{\ell})]|_{\rho_0} \sum_{n\geqslant 1} \frac{(-\boldsymbol{\ell}\cdot\partial_{\mathbf{x}})^n}{n!} \delta\rho, \tag{25}$$

where $p'_\rho = dp_\rho/d\rho$. We infer the dynamics of the Fourier modes $\delta\rho_{\mathbf{k}}(t) = \int \delta\rho(\mathbf{x},t)e^{i\mathbf{k}\cdot\mathbf{x}}d\mathbf{x}$ as

$$\begin{aligned}\partial_t \delta\rho_{\mathbf{k}} &= \nu\delta\rho_{\mathbf{k}} \int d\boldsymbol{\ell}[p_\rho(\boldsymbol{\ell}) + \rho_0 p'_\rho(\boldsymbol{\ell})]|_{\rho_0} \sum_{n\geqslant 1} \frac{(i\boldsymbol{\ell}\cdot\mathbf{k})^n}{n!} \\ &= \nu\delta\rho_{\mathbf{k}} \int d\boldsymbol{\ell}[p_\rho(\boldsymbol{\ell}) + \rho_0 p'_\rho(\boldsymbol{\ell})]|_{\rho_0} (e^{i\boldsymbol{\ell}\cdot\mathbf{k}} - 1) \\ &= \nu\delta\rho_{\mathbf{k}}\left[\left(1 + \rho_0\frac{d}{d\rho}\right)\langle e^{i\boldsymbol{\ell}\cdot\mathbf{k}}\rangle|_{\rho_0} - 1\right].\end{aligned} \tag{26}$$

Assuming that the jump distribution does not have any angular dependence, so that only even moments of $\boldsymbol{\ell}$ are nonzero, we deduce the following criterion for the occurrence long-wavelength instabilities:

$$\left(1 + \rho_0\frac{d}{d\rho}\right)\langle \ell^2\rangle < 0. \tag{27}$$

This instability criterion does not depend on the jump rate ν, as expected in the absence of any other time to compare it to.

To assess the existence of phase separation, we perform simulations in a finite 2D box with periodic boundaries conditions. For simplicity, we choose the jump length to be fixed, $p_\rho(\boldsymbol{\ell}) = \delta(|\boldsymbol{\ell}| - a(\rho))$, where a depends on the local density as

$$a(\rho) = a_{\rm M} + \frac{a_{\rm m} - a_{\rm M}}{2}\left[1 + \tanh\frac{\rho - \rho_{\rm m}}{\Delta\rho}\right]. \tag{28}$$

The typical values at low and high densities are $a_{\rm M}$ and $a_{\rm m}$, respectively. In practice, the local density is determined within a fixed radius surrounding each particle. For appropriate values of parameters, one indeed observes a complete phase separation between dense and dilute regions, as reported in Fig. 3.

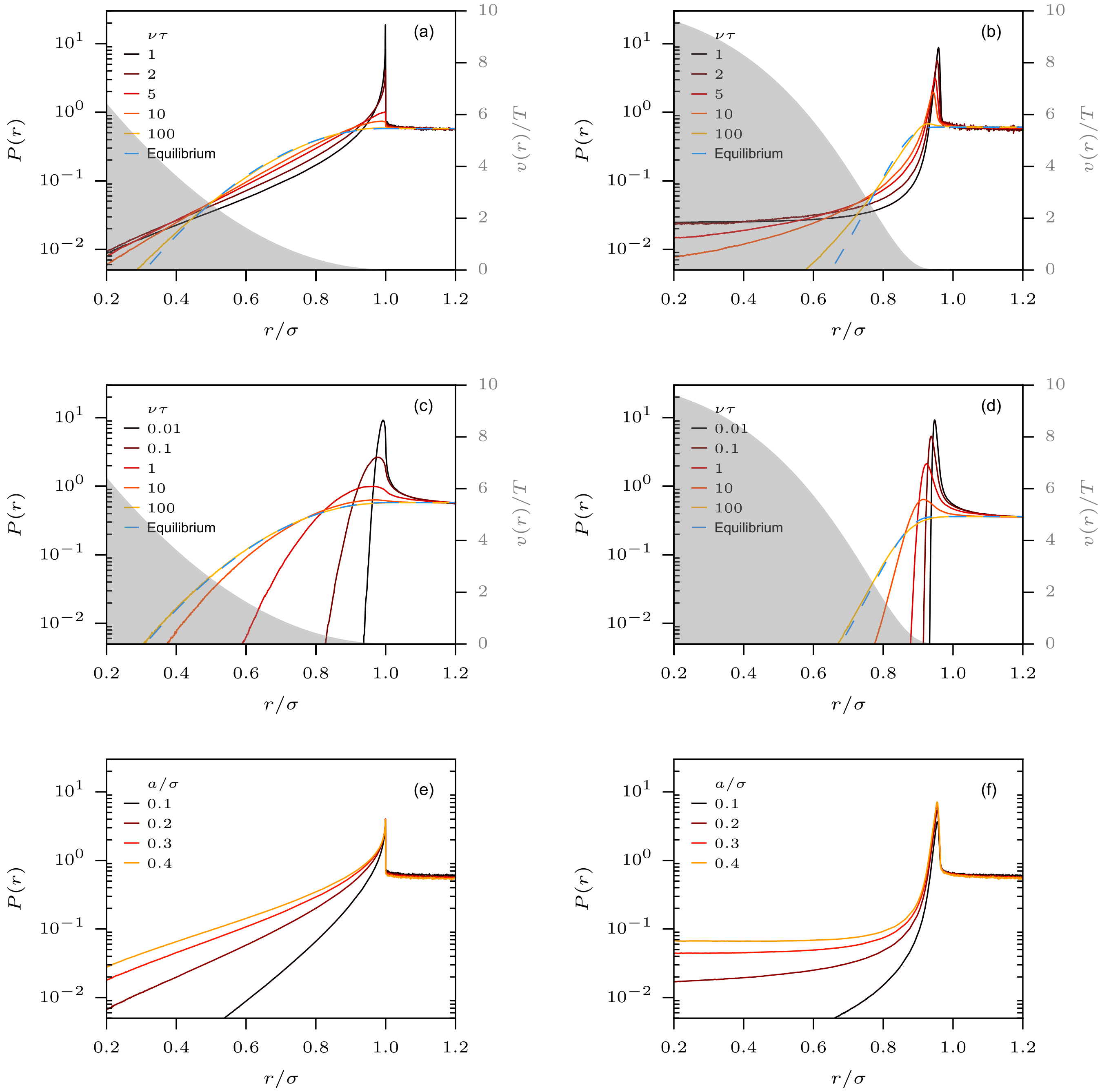

FIG. 2. Radial distribution of particle position away from the obstacle center. The shaded region represents the obstacle potential: (a), (c), and (e) harmonic $v(r) = \varepsilon(1 - r/\sigma)^2$ and (b), (d), and (f) exponential $v(r) = \varepsilon \exp\{-1/[(\sigma/r)^2 - 1]\}$. The blue dashed line in (a)–(d) refers to the equilibrium limit. The remarkable feature is the accumulation of particles in the vicinity of the obstacle without the need to invoke memory effects, at a location where the equilibrium profile is featurelessly flat. (a) and (b) Non-Gaussian white noise for different values of $\nu\tau$, where $\tau = \gamma\sigma^2/\varepsilon$. The parameters are $T = 1$, $\gamma = 1$, $\varepsilon = 10$, $\sigma = 1$, and $m = 10^{-4}$. (c) and (d) Exponentially correlated Gaussian noise with persistence time $1/\nu$ (AOUPs). The parameters are the same as in (a) and (b). (e) and (f) Non-Gaussian white noise for different values of a/σ at fixed $\nu\tau = 2$. Since the temperature $T \sim \nu a^2$ varies, the potential $v(r)/T$ is not drawn here. All other parameters are the same as in (a) and (b).

B. Pairwise forces and effective attraction

To study the interplay between pairwise forces and non-Gaussian noises, we have performed 2D simulations of particles interacting via a two-body repulsive potential $U = \sum_{i\neq j} v(\mathbf{r}_i - \mathbf{r}_j)$, where $v(r) = \varepsilon[(\sigma/r)^{12} - 2(\sigma/r)^6]\Theta(\sigma - r)$ [72]. For similar interaction potentials, RTPs, ABPs, and AOUPs all display MIPS [5,19,51,71]. Our goal is to sort out the relative contributions of the persistence, on the one hand, and non-Gaussian statistics, on the other, which are typically intertwined in active particles.

We work at fixed particle density $\rho_0 = 0.6$, for which ABPs exhibit MIPS at large persistence, and we consider a fixed jump length $p(\boldsymbol{\ell}) = \delta(|\boldsymbol{\ell}| - a)$. The equilibrium limit,

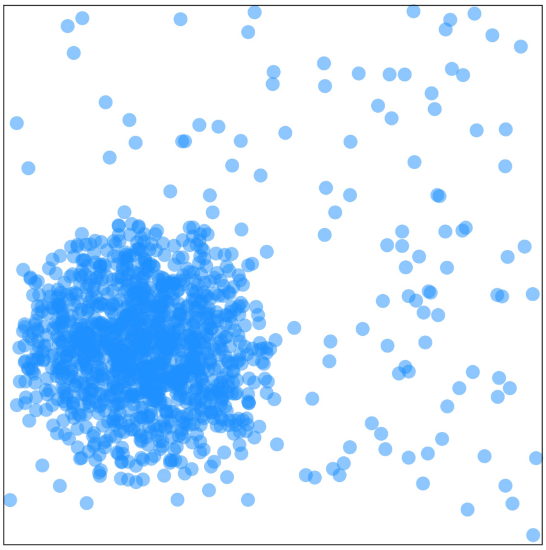

FIG. 3. Phase separation for density-dependent jumping length $a(\rho)$, as given in (28), in a 2D box of size L, with periodic boundary conditions. For every particle, the blue circle denotes the area over which the local density is computed. The parameters are $\rho_0 = 0.6$, $\rho_{\rm m} = 0.6$, $\Delta\rho_0 = 0.006$, $L = 40$, $a_{\rm M} = 10$, and $a_{\rm m} = 1$.

corresponding to a Gaussian noise, is achieved as the hopping range $a \to 0$ and the hopping frequency $\nu \to \infty$ while keeping $T \sim \nu a^2$ fixed. Hence, we progressively drift away from equilibrium by slowing down the kicks at fixed temperature, namely, by either reducing ν or increasing a at fixed νa^2. In addition, to prevent particles from crossing each other when they should not, we use a finite yet small value of mass m. Note that this requires using extremely small time steps, which significantly increases numerical cost.

The static structure is characterized by the two-body density correlation $g(\mathbf{r}-\mathbf{r}') = (1/\rho_0^2)\langle\rho(\mathbf{r})\rho(\mathbf{r}')\rangle$. We observe that the first two peaks of g, close to $r = \{\sigma, 2\sigma\}$, increase when departing from the equilibrium regime, as shown in Fig. 4. This suggests an increase of local order compatible with the emergence of motility-induced clustering. Note, however, that for the times and sizes accessible to our numerics, we could not observe a complete phase separation. We defer an extensive analysis of the corresponding finite-size effects to future works.

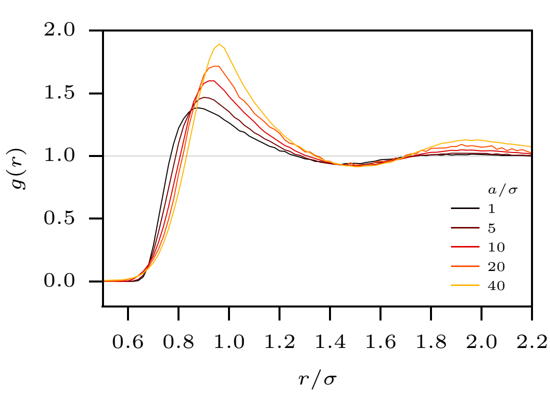

FIG. 4. Density pair correlation g as a function of interparticle distance r scaled by particle diameter σ. The hopping range a is varied at constant $\nu a^2 = 1$. Note that the first and second peaks become all the more pronounced as we depart from equilibrium. The parameters are $\rho_0 = 0.6$, $m = 10^{-3}$, $L = 40$, $\gamma = 1$, $\sigma = 1$, and $\varepsilon = 10^2$.

C. Generalized Dean-Kawasaki equation

To describe collective effects, we now analyze the statistics of the fluctuating particle density ρ for pairwise forces. The dynamics of ρ can be obtained in the same vein as for a Gaussian white noise by using Itô calculus [52,53], yet this derivation must be greatly revised due to the non-Gaussian nature of the noise. This was considered two decades ago in the mathematical literature [34–36]. Appendix A gives the proper discretization scheme in physical terms, recently revived in [45], which is consistent with differential calculus for a generic non-Gaussian noise.

The corresponding chain rule then leads to

$$\begin{aligned}\partial_t\rho &= -\partial_{\mathbf{x}}\cdot\sum_i \frac{d\mathbf{r}_i}{dt} * \delta(\mathbf{x}-\mathbf{r}_i)\\ &= -\partial_{\mathbf{x}}\cdot\sum_i \big(-\gamma^{-1}\partial_{\mathbf{r}_i}U + \boldsymbol{\eta}_i\big) * \delta(\mathbf{x}-\mathbf{r}_i),\end{aligned}\tag{29}$$

where the multiplicative noise signaled by the $*$ product must be understood in terms of $\Delta\rho(\mathbf{x},t) = \rho(\mathbf{x},t+\Delta t) - \rho(\mathbf{x},t)$ and $\Delta\boldsymbol{\eta}_i = \int_t^{t+\Delta t} d\tau\, \boldsymbol{\eta}_i(\tau)$ as

$$\begin{aligned}\Delta\rho &= -\partial_{\mathbf{x}}\cdot\sum_i\bigg[-\gamma^{-1}\partial_{\mathbf{r}_i}U\delta(\mathbf{x}-\mathbf{r}_i)\\ &\quad + \frac{e^{\Delta\boldsymbol{\eta}_i\cdot\partial_{\mathbf{r}_i}}-1}{\Delta\boldsymbol{\eta}_i\cdot\partial_{\mathbf{r}_i}}\delta(\mathbf{x}-\mathbf{r}_i)\Delta\boldsymbol{\eta}_i\bigg]\\ &= -\partial_{\mathbf{x}}\cdot\sum_i\bigg[-\gamma^{-1}\partial_{\mathbf{r}_i}U\delta(\mathbf{x}-\mathbf{r}_i)\\ &\quad + \frac{e^{-\Delta\boldsymbol{\eta}_i\cdot\partial_{\mathbf{x}}}-1}{-\Delta\boldsymbol{\eta}_i\cdot\partial_{\mathbf{x}}}\delta(\mathbf{x}-\mathbf{r}_i)\Delta\boldsymbol{\eta}_i\bigg].\end{aligned}\tag{30}$$

This allows us to determine the Kramers-Moyal coefficients $\{K^{(k)}\}$, defined by

$$K^{(k)}(\mathbf{x}_1,\ldots,\mathbf{x}_k) = \lim_{\Delta t\to 0}\frac{\langle\Delta\rho(\mathbf{x}_1)\cdots\Delta\rho(\mathbf{x}_k)\rangle}{\Delta t}.\tag{31}$$

Once these coefficients are known, we can directly write an Itô-discretized stochastic equation for ρ, in the form

$$\partial_t\rho = K^{(1)} + \mathcal{N},\tag{32}$$

where $\mathcal{N}$ denotes noise. Here the white noise is non-Gaussian, with zero mean and cumulant amplitude given by $K^{(k)}$ for $k \geqslant 2$. A tedious but straightforward calculation leads to

$$\begin{aligned}K^{(1)}(\mathbf{x}) &= \gamma^{-1}\partial_{\mathbf{x}}\cdot\bigg[\rho(\mathbf{x},t)\int_{\mathbf{y}}\partial_{\mathbf{x}}v(\mathbf{x}-\mathbf{y})\rho(\mathbf{y},t)\bigg]\\ &\quad - \partial_{\mathbf{x}}\cdot\sum_{p=0}^{\infty}\frac{(-1)^p\kappa^{(p+1)}}{(p+1)!}\partial_{\mathbf{x}}^p\rho\end{aligned}\tag{33}$$

and, for $k \geqslant 2$,

$$K^{(k)} = (-1)^k \partial_{\mathbf{x}_1} \cdots \partial_{\mathbf{x}_k} \sum_{p_1,\dots,p_k} \frac{(-1)^{p_1+\dots+p_k} K^{(p_1+\dots+p_k+k)}}{(p_1+1)!\cdots(p_k+1)!} \times \partial_{\mathbf{x}_1}^{p_1} \cdots \partial_{\mathbf{x}_k}^{p_k} \rho \delta(\mathbf{x}_1 - \mathbf{x}_2) \cdots \delta(\mathbf{x}_{k-1} - \mathbf{x}_k). \tag{34}$$

Equations (32)–(34) can be viewed as the non-Gaussian generalization of the Dean-Kawasaki equation. Again, we stress that, by construction, it is written in Itô form. A somewhat more physically appealing form reads

$$\partial_t \rho = -\partial_{\mathbf{x}} \cdot \mathbf{j}, \tag{35}$$

where the fluctuating current $\mathbf{j}$ is given by

$$\mathbf{j}(\mathbf{x}, t) = -\mathbf{D}_{\mathbf{x}} \rho - \frac{1}{\gamma} \rho(\mathbf{x}, t) \int_{\mathbf{y}} \partial_{\mathbf{x}} v(\mathbf{x} - \mathbf{y}) \rho(\mathbf{y}, t) + \mathcal{N}. \tag{36}$$

The notation $\mathbf{D}_{\mathbf{x}}$, which generalizes the simple diffusive transport, has already been introduced in (8).

One can reformulate the Langevin equations (32)–(34) in terms of a Martin–Siggia–Rose–Janssen–De Dominicis path integral. We demonstrate in Appendix B that the corresponding dynamical action can be written as

$$S = \int_{\mathbf{x},t} \left[\bar{\rho} \partial_t \rho + \frac{1}{\gamma} \partial_{\mathbf{x}} \bar{\rho} \cdot \int_{\mathbf{y}} \rho(\mathbf{x}, t) \partial_{\mathbf{x}} v(\mathbf{x} - \mathbf{y}) \rho(\mathbf{y}, t) \right] - \nu \int_{\mathbf{x},\boldsymbol{\ell},t} \rho(\mathbf{x}, t) [e^{\bar{\rho}(\mathbf{x}+\boldsymbol{\ell},t) - \bar{\rho}(\mathbf{x},t)} - 1] p(\boldsymbol{\ell}). \tag{37}$$

The Itô discretization ensures that one does not have to deal with any Jacobian. We treat here ρ as a well-behaved field of integration, though it is *a priori* a sum of δ functions centered around each particle. A formal proof that this is indeed legitimate for an ideal gas of Brownian particles has been given in [73]. While (37) is fully general, it is also remarkably complex. As a consistency check, one can proceed directly from a Doi-Peliti approach using the second-quantized operators a and $\bar{a}$ [74,75], where the contribution for the particle hops reads

$$\nu \int_{\mathbf{x},\boldsymbol{\ell}} p(\boldsymbol{\ell}) [\bar{a}(\mathbf{x} + \boldsymbol{\ell}, t) - \bar{a}(\mathbf{x}, t)] a(\mathbf{x}, t). \tag{38}$$

Using the density operators ρ and $\bar{\rho}$ introduced by Grassberger [76] as $a = e^{-\bar{\rho}} \rho$ and $\bar{a} = e^{\bar{\rho}}$, one ends up with the same dynamic action (37), as detailed in Appendix B.

D. Density correlations: Perturbative treatment

The Langevin equations (32)–(34), or alternatively the dynamic action (37), provide a systematic toolbox to study k-point correlations $\rho^{(k)}$ defined as

$$\rho^{(k)}(\mathbf{x}_1, \dots, \mathbf{x}_k) = \left\langle \sum_{i_1 \neq \dots \neq i_k} \delta(\mathbf{x}_1 - \mathbf{r}_{i_1}) \cdots \delta(\mathbf{x}_k - \mathbf{r}_{i_k}) \right\rangle \tag{39}$$

through a BBGKY hierarchy [54]. For instance, the dynamics of the first nontrivial correlations can be written for $t' < t$ as

$$\partial_t \langle \rho(\mathbf{x}', t') \rho(\mathbf{x}, t) \rangle = \partial_{\mathbf{x}} \cdot \mathbf{D}_{\mathbf{x}} \langle \rho(\mathbf{x}', t') \rho(\mathbf{x}, t) \rangle + \gamma^{-1} \partial_{\mathbf{x}} \cdot \int_{\mathbf{y}} \partial_{\mathbf{x}} v(\mathbf{x} - \mathbf{y}) \langle \rho(\mathbf{x}', t') \rho(\mathbf{x}, t) \rho(\mathbf{y}, t) \rangle. \tag{40}$$

In the limit $t' \to t^- \to \infty$, using

$$\begin{aligned} \langle \rho(\mathbf{x}) \rho(\mathbf{x}') \rangle &= \rho^{(2)}(\mathbf{x} - \mathbf{x}') + \rho_0 \delta(\mathbf{x} - \mathbf{x}'), \\ \langle \rho(\mathbf{x}') \rho(\mathbf{x}) \rho(\mathbf{y}) \rangle &= \rho^{(3)}(\mathbf{x}, \mathbf{x}', \mathbf{y}) + \delta(\mathbf{x} - \mathbf{x}') \rho^{(2)}(\mathbf{x}, \mathbf{y}) \\ &\quad + \delta(\mathbf{x} - \mathbf{y}) \rho^{(2)}(\mathbf{x}, \mathbf{x}') + \delta(\mathbf{x}' - \mathbf{y}) \rho^{(2)}(\mathbf{x}, \mathbf{y}) \\ &\quad + \delta(\mathbf{x} - \mathbf{x}') \delta(\mathbf{x} - \mathbf{y}) \delta(\mathbf{x}' - \mathbf{y}) \rho^{(1)}(\mathbf{x}), \end{aligned} \tag{41}$$

we arrive at

$$0 = \partial_{\mathbf{x}} \cdot [\mathbf{D}_{\mathbf{x}} \rho^{(2)}(\mathbf{x}, \mathbf{x}') + \gamma^{-1} \rho^{(2)}(\mathbf{x}, \mathbf{x}') \partial_{\mathbf{x}} v(\mathbf{x} - \mathbf{x}')] + \gamma^{-1} \partial_{\mathbf{x}} \cdot \int_{\mathbf{y}} \partial_{\mathbf{x}} v(\mathbf{x} - \mathbf{y}) \rho^{(3)}(\mathbf{x}, \mathbf{x}', \mathbf{y}). \tag{42}$$

This can be regarded as the non-Gaussian generalization of the Born-Green-Yvon (BGY) equation [77,78], originally introduced for Hamiltonian dynamics.

We now consider the low-density regime where correlations of order $k > 2$ are negligible and analytical progress is possible: The generalized BGY equation (42) then reduces to an equation for pair correlations $g(r) = \rho^{(2)}(r)/\rho_0^2$ only. For a generic interaction potential $v(\mathbf{r})$, no exact solution can be found. Using the Boltzmann-Gibbs weight as a reference distribution, we expand the stationary state in powers of the non-Gaussianity of the applied noise. A similar expansion was recently carried out within the framework of quantitative finance [39] for a single degree of freedom. Scaling position as $\mathbf{r}' = \mathbf{r}/\sigma$, where σ is a typical length scale such as the range of interactions, we get

$$0 = \partial_{\mathbf{r}'} \cdot (g \partial_{\mathbf{r}'} v) + T \partial_{\mathbf{r}'}^2 \left[1 - c_{d,\alpha} \left(\frac{a}{\sigma} \right)^2 \partial_{\mathbf{r}'}^2 + O\left(\frac{a}{\sigma} \right)^4 \right] g, \tag{43}$$

where $c_{d,\alpha}$ is a dimensionless coefficient which depends on the spatial dimension d and on the jump parameter α. Using the Boltzmann weight as a reference distribution, we expand g in powers of a at fixed $T \sim \nu a^2$ as $g(\mathbf{r}') \sim e^{-(v(\mathbf{r}') + w(\mathbf{r}'))/T}$, where $w \to 0$ in the Gaussian limit. We deduce that $w = O(a/\sigma)^2$ and that it satisfies

$$\frac{\partial_{\mathbf{r}'} w}{c_{d,\alpha}} = \left(\frac{a}{\sigma} \right)^2 \left[\partial_{\mathbf{r}'} - \frac{(\partial_{\mathbf{r}'} v)}{T} \right] \left[\frac{(\partial_{\mathbf{r}'} v)^2}{T} - \Delta_{\mathbf{r}'} v \right]. \tag{44}$$

For a simple repulsive potential $v(\mathbf{r}) = \varepsilon(\sigma/r)^{12}$, we find

$$\frac{w(\mathbf{r})}{c_{d,\alpha}} = 24\varepsilon \left(\frac{a}{\sigma} \right)^2 \left[\frac{d - 14}{2} \left(\frac{\sigma}{r} \right)^{14} + \frac{3(d - 40)}{13} \frac{\varepsilon}{T} \left(\frac{\sigma}{r} \right)^{26} - \frac{36}{19} \left(\frac{\varepsilon}{T} \right)^2 \left(\frac{\sigma}{r} \right)^{38} \right], \tag{45}$$

where we have used $\Delta_{\mathbf{r}} v = r^{1-d} \partial_r (r^{d-1} \partial_r v)$. The leading contribution induces an attractive interaction at distances of the order of σ, with a strength proportional to T/ν, similarly to AOUPs with persistence $1/\nu$ [22]. This suggests that effective attractive interactions are indeed to be expected in a dilute limit and for mildly non-Gaussian noise. This is consistent with our numerical observations in Fig. 4.

IV. CONCLUSION

The dynamical evolution of an active particle is often modeled after a Langevin equation in which the noise source drives the particle away from equilibrium by displaying persistent properties along with non-Gaussian statistics [6,79,80]. In this work, we have focused on the purely non-Gaussian effects of the active noise by discarding all memory effects. We have provided analytical results for the position distribution of a single particle in a harmonic trap. We have also reported some numerical evidence of accumulation at the boundaries of an obstacle. This supports that non-Gaussian effects alone can yield effective attraction from bare repulsion, similarly to the case of persistent particles [21,58,63,81].

Considering particles interacting via quorum sensing, we reported the existence of a phase separation analogous to MIPS [3,7]. For pairwise forces, the effective attraction enhances spontaneous clustering, as testified by density correlations. However, within the explored range of parameters, we have not witnessed any phase separation for such interactions. To investigate collective effects, we have derived the stochastic density dynamics by extending standard procedures to non-Gaussian noise [52,53]. In the dilute limit and for weakly non-Gaussian noise, a systematic expansion has confirmed the emergence of effective attraction from bare repulsive interactions, in line with our numerical results.

When driven by a non-Gaussian white noise, the dynamics in the presence of interactions operates far from equilibrium by breaking time-reversal symmetry. It would be interesting to investigate deeper the consequences for a ratchet, where a current develops spontaneously in an asymmetric periodic potential, by analogy with persistent noises [82–85]. Moreover, the properties of a heat engine subject to a non-Gaussian white noise could be explored, following [45,86,87]. In particular, the role of particle interactions in the performance of ratchets and engines, studied recently for driven and persistent particles [88,89], calls for deeper investigation in the non-Gaussian case.

ACKNOWLEDGMENTS

We warmly acknowledge discussions with Kiyoshi Kanazawa and Tomohiko Sano. During this work F.v.W. benefited from support from a Yukawa Institute visiting professorship and É.F. benefited from YITP financial support. We also acknowledge financial support from IRSES SoftActive. H.H. acknowledges financial support by the Grant-in-Aid of MEXT for Scientific Research (Grant No. 16H04025). F.v.W. benefited from the support of the Institut Universitaire de France. J.T. acknowledges support from ANR grant Bactterns. É.F. benefits from an Oppenheimer Research Fellowship from the University of Cambridge and a Junior Research Fellowship from St. Catherine's College.

APPENDIX A: DISCRETIZATION ISSUES

This appendix is devoted to presenting, in a way familiar to the chemist or the physicist [55–57] and based on the Kramers-Moyal expansion, the rules of stochastic calculus involving white but non-Gaussian noise. These rules are well known to the mathematics community, which has its own language to express these [34–36] (see also [38] for a more recent exposition). The present appendix is also an alternative to the more recent presentation by Kanazawa *et al.* [45]. To make things as pedagogical as possible, we begin with a general Langevin equation for a process $x(t)$ evolving according to

$$\frac{dx}{dt} = A(x) + B(x)\eta(t), \tag{A1}$$

where the noise η is characterized by its cumulants

$$\langle\eta(t_1)\cdots\eta(t_n)\rangle = \kappa^{(n)}\delta(t_1 - t_2)\cdots\delta(t_{n-1} - t_n). \tag{A2}$$

The experienced reader knows that, as such, Eq. (A1) needs to be supplemented by a discretization rule (without which it is meaningless) and the product $B\eta$ is best written using a warning sign $B * \eta$. By definition, the Itô rule for understanding (A1) reads

$$\Delta x = x(t+\Delta t) - x(t) = A(x(t))\Delta t + B(x(t))\int_t^{t+\Delta t} d\tau\, \eta(\tau), \tag{A3}$$

where Δt is an infinitesimal discretization scale. In the following, we will often use the notation $\Delta\eta = \int_t^{t+\Delta t} d\tau\, \eta(\tau)$. It is easy to realize that

$$\langle(\Delta\eta)^k\rangle = \kappa^{(k)}\Delta t + o(\Delta t) \tag{A4}$$

and thus, as $\Delta t \to 0$,

$$\frac{\langle\Delta x\rangle}{\Delta t} = A, \quad \frac{\langle\Delta x^k\rangle}{\Delta t} = [B(x)]^k\kappa^{(k)} \quad \text{for } k \geqslant 2 \tag{A5}$$

and this explains the form of the master or Fokker-Planck equation (7) obtained for $B = 1$ and $A = -\partial_x U$. Of course, depending on context, other discretization rules could be implemented on Eq. (A1) and they would lead to different physical processes with different Fokker-Planck equations. For instance, the Stratonovich rule would read

$$\begin{aligned}\Delta x &= x(t+\Delta t) - x(t) = A\Delta t + B(x(t) + \tfrac{1}{2}\Delta x)\Delta\eta \\ &= A\Delta t + B\Delta\eta + \tfrac{1}{2}B'\Delta x\Delta\eta + \cdots \\ &= A\Delta t + B\Delta\eta + \tfrac{1}{2}B'B\Delta\eta^2 + \cdots,\end{aligned} \tag{A6}$$

where the ellipses stand for terms that are of lower order in the $\Delta t \to 0$ limit only when the noise is Gaussian. For a Gaussian white noise, the Stratonovich rule ensures that the chain rule is consistent with stochastic calculus. In other words, given an arbitrary function $f(x)$, with the Stratonovich rule one may safely write that

$$\frac{df}{dt} = f'(x(t))\frac{dx}{dt} = f'(A + B * \eta) = f'A + (f'B) * \eta, \tag{A7}$$

where $(f'B) * \eta$ on the right-hand side is to be understood in the Stratonovich sense as long as $B * \eta$ in the evolution of $x(t)$ is as well. However, (A7) only holds for the Stratonovich discretization and for η a Gaussian white noise. This is not the case anymore for a generic non-Gaussian white noise. Another discretization rule plays this special role of being transparent to differential calculus. It is defined as

$$\begin{aligned}\Delta x &= x(t+\Delta t) - x(t)\\ &= A\Delta t + \frac{e^{B(x)\Delta\eta(d/dx)} - 1}{B(x)\Delta\eta(d/dx)} B(x)\Delta\eta,\end{aligned} \tag{A8}$$

where the t argument in $x(t)$ was omitted. Note that truncating the right-hand side in (A8) to order $\Delta\eta^2$ leads to one recovering (A6). To leading order in Δt and for a Gaussian white noise, both discretization prescriptions are identical. Now let us prove that the prescription (A8) is indeed transparent to differential calculus in the sense that differential calculus can blindly be used. We consider a function $f(x(t))$ and ask whether we have

$$\begin{aligned}\frac{df}{dt} &= f'(x(t)) * \frac{dx}{dt}\\ &= f' * (A + B * \eta) = f'A + (f'B) * \eta.\end{aligned} \tag{A9}$$

Introducing a discretization scale Δt, we must evaluate $\Delta f = f(x+\Delta x) - f(x)$ in two ways. We introduce the generalized translation operator $\hat{T}_B$ defined by $\hat{T}_B[w] = \frac{e^{\Delta\eta B(d/dx)}-1}{\Delta\eta B(d/dx)} w(x)$. We begin with

$$\begin{aligned}\Delta f &= f(x+\Delta x) - f(x)\\ &= f(x + A\Delta t + \hat{T}_B[B\Delta\eta]) - f(x),\end{aligned} \tag{A10}$$

which we want to compare with the expression that would be deduced from the blind application of the chain rule

$$\begin{aligned}\Delta f &= f'A\Delta t + \int_t^{t+\Delta t} (f'B) * \eta\\ &= f'A\Delta t + \hat{T}_B[f'B\Delta\eta].\end{aligned} \tag{A11}$$

If we can prove that Eqs. (A10) and (A11) are actually identical, then we will have established our result. First we note that for any function f,

$$\hat{T}_B[f'B\Delta\eta] = (e^{B\Delta\eta(d/dx)} - 1)f, \tag{A12}$$

which also means, for $f(x) = x$, that $\hat{T}_B[B\Delta\eta] = (e^{B\Delta\eta(d/dx)} - 1)x$, and we are left with the following identity between Eqs. (A10) and (A11) to prove as $\Delta t \to 0$:

$$f(A\Delta t + e^{B\Delta\eta(d/dx)}x) = f'A\Delta t + e^{B\Delta\eta(d/dx)} f. \tag{A13}$$

We first remark that, on the left-hand side,

$$\begin{aligned}&f(A\Delta t + e^{B\Delta\eta(d/dx)}x)\\ &\quad= f(e^{B\Delta\eta(d/dx)}x) + f'(e^{B\Delta\eta(d/dx)}x)A\Delta t + O(\Delta t^2)\\ &\quad= f(e^{B\Delta\eta(d/dx)}x) + f'(x)A\Delta t + O(\Delta t^2).\end{aligned} \tag{A14}$$

We now prove the following exact identity (valid at arbitrary Δt):

$$f(e^{B\Delta\eta(d/dx)}x) = e^{B\Delta\eta(d/dx)} f(x). \tag{A15}$$

To do so we introduce the variable y such that $\frac{dx}{dy} = B\Delta\eta$ and write $x = g(y)$ where we do not need the explicit form of g. In terms of the y variable, Eq. (A15) becomes

$$f(e^{d/dy} g(y)) = e^{d/dy} f(g(y)). \tag{A16}$$

Using that for any function $h(y)$, $e^{d/dy}h(y) = h(y+1)$, which we apply to $h(y) = g(y)$ and to $h(y) = f(g(y))$, we have thus proved Eq. (A16), which in turn establishes Eq. (A15) and thus ensures the equality between Eqs. (A10) and (A11). Hence, for a non-Gaussian white noise, the prescription rule (A8) allows for the blind use of differential calculus.

APPENDIX B: DYNAMIC ACTION

Our goal is to obtain an explicit expression of the dynamic action S in terms of the jump distribution p of the non-Gaussian noise. Following standard procedures, the action associated with the dynamics of the position density in (35) and (36) can be written as

$$\begin{aligned}S = \int_{\mathbf{x},t} &\left[\bar{\rho}\partial_t\rho + \frac{1}{\gamma}\partial_{\mathbf{x}}\bar{\rho}\cdot\int_{\mathbf{y}}\rho(\mathbf{x},t)v(\mathbf{x}-\mathbf{y})\rho(\mathbf{y},t)\right]\\ &- \sum_{n=1}^{\infty}\frac{1}{n!}\int_{\mathbf{x}^n,t}\bar{\rho}(\mathbf{x}_1,t)\cdots\bar{\rho}(\mathbf{x}_n,t)\langle\xi(\mathbf{x}_1,t)\cdots\xi(\mathbf{x}_n,t)\rangle_c,\end{aligned} \tag{B1}$$

where the noise term ξ is written in terms of the microscopic noises $\{\boldsymbol{\eta}_i\}$ and $\rho_i(\mathbf{x},t) = \delta(\mathbf{x} - \mathbf{x}_i(t))$ as

$$\xi(\mathbf{x},t) = -\sum_{i=1}^{N}\nabla[\boldsymbol{\eta}_i(t)\rho_i(\mathbf{x},t)]. \tag{B2}$$

The noise cumulants can be expressed in terms of the variation of density $\Delta\rho_j = \Delta\rho(\mathbf{x}_j,t)$ during a time Δt in the absence of potential as

$$\langle\xi(\mathbf{x}_1,t)\cdots\xi(\mathbf{x}_n,t)\rangle_c = \lim_{\Delta t\to 0}\frac{\langle\Delta\rho_1\cdots\Delta\rho_2\rangle}{\Delta t}. \tag{B3}$$

The density variation in the absence of potential is given by

$$\Delta\rho(\mathbf{x},t) = \sum_{i=1}^{N}\sum_{k=1}^{\infty}\frac{(-1)^k}{k!}[\Delta\boldsymbol{\eta}_i(t)\cdot\nabla]^k\rho_i(\mathbf{x},t). \tag{B4}$$

The product of the density variations follows as

$$\begin{aligned}\langle\Delta\rho_1\cdots\Delta\rho_n\rangle = \nu &\sum_{k^n,\alpha^n,i^n}\left\langle\Delta\eta_{i_1\alpha_1}^{k_1}\cdots\Delta\eta_{i_n\alpha_n}^{k_n}\right\rangle\\ &\times\prod_{j=1}^{n}\frac{(-1)^{k_j}}{k_j!}\left(\partial_{i_j\alpha_j}\right)^{k_j}\rho_{i_j}(\mathbf{x}_j,t),\end{aligned} \tag{B5}$$

where the elements in $\alpha^n = \{\alpha_1,\ldots,\alpha_n\}$ run from 1 to d, the ones in $k^n = \{k_1,\ldots,k_n\}$ from 1 to ∞, and the ones in $i^n = \{i_1,\ldots,i_n\}$ from 1 to N. Substituting the expression for the noise cumulants, we get

$$\langle \Delta\rho_1 \cdots \Delta\rho_n \rangle = \nu \Delta t \int \sum_{k_1=1}^{\infty} \frac{1}{k_1!} \left(-\sum_{\alpha_1=1}^{d} \ell_{\alpha_1} \partial_{1\alpha_1} \right)^{k_1} \cdots \sum_{k_n=1}^{\infty} \frac{1}{k_n!} \left(-\sum_{\alpha_n=1}^{d} \ell_{\alpha_n} \partial_{n\alpha_n} \right)^{k_n}$$
$$\times \sum_{i=1}^{N} \rho_i(\mathbf{x}_1, t) \cdots \rho_i(\mathbf{x}_n, t) p(\boldsymbol{\ell}) d\boldsymbol{\ell} + O(\Delta t^2). \tag{B6}$$

We use the properties of the Dirac δ function to simplify the last sum in Eq. (B6) as

$$\sum_{i=1}^{N} \rho_i(\mathbf{x}_1, t) \cdots \rho_i(\mathbf{x}_n, t) = \delta(\mathbf{x}_1 - \mathbf{x}_2) \cdots \delta(\mathbf{x}_{n-1} - \mathbf{x}_n) \rho(\mathbf{x}_1, t), \tag{B7}$$

yielding

$$\langle \Delta\rho_1 \cdots \Delta\rho_n \rangle = \nu \Delta t \int \left[\prod_{j=1}^{n} \sum_{k=1}^{\infty} \frac{(-\boldsymbol{\ell} \cdot \nabla_j)^k}{k!} \right] \rho(\mathbf{x}_1, t) \delta(\mathbf{x}_1 - \mathbf{x}_2) \cdots \delta(\mathbf{x}_{n-1} - \mathbf{x}_n) p(\boldsymbol{\ell}) d\boldsymbol{\ell} + O(\Delta t^2)$$
$$= \nu \Delta t \int \left[\prod_{j=1}^{n} \left(e^{-\boldsymbol{\ell} \cdot \nabla_j} - 1 \right) \right] \rho(\mathbf{x}_1, t) \delta(\mathbf{x}_1 - \mathbf{x}_2) \cdots \delta(\mathbf{x}_{n-1} - \mathbf{x}_n) p(\boldsymbol{\ell}) d\boldsymbol{\ell} + O(\Delta t^2). \tag{B8}$$

When substituting Eq. (B8) in Eq. (B1), a term of the form

$$\int_{\mathbf{x}^n} \bar{\rho}(\mathbf{x}_1, t)(e^{-\boldsymbol{\ell} \cdot \nabla_1} - 1) \left[\rho(\mathbf{x}_1, t) \prod_{j=2}^{n} \bar{\rho}(\mathbf{x}_j, t)(e^{-\boldsymbol{\ell} \cdot \nabla_j} - 1) \delta(\mathbf{x}_1 - \mathbf{x}_j) \right]$$
$$= \int_{\mathbf{x}^n} \rho(\mathbf{x}_1, t) \left[\prod_{j=2}^{n} \delta(\mathbf{x}_1 - \mathbf{x}_j)(e^{\boldsymbol{\ell} \cdot \nabla_j} - 1) \bar{\rho}(\mathbf{x}_j, t) \right] (e^{\boldsymbol{\ell} \cdot \nabla_1} - 1) \bar{\rho}(\mathbf{x}_1, t)$$
$$= \int_{\mathbf{x}} \rho(\mathbf{x}, t) [(e^{\boldsymbol{\ell} \cdot \nabla_{\mathbf{x}}} - 1) \bar{\rho}(\mathbf{x}, t)]^n \tag{B9}$$

appears, where we have integrated by parts with respect to $\mathbf{x}^n$ to get the second line and we have integrated over $\mathbf{x}^{n-1} = \{\mathbf{x}_2, \ldots, \mathbf{x}_n\}$ to obtain the third one. The dynamic action follows as

$$S = \int_{\mathbf{x},t} \left[\bar{\rho} \partial_t \rho + \frac{1}{\gamma} \partial_{\mathbf{x}} \bar{\rho} \cdot \int_{\mathbf{y}} \rho(\mathbf{x}, t) \partial_{\mathbf{x}} v(\mathbf{x} - \mathbf{y}) \rho(\mathbf{y}, t) \right] - \nu \int_{\mathbf{x},\boldsymbol{\ell},t} \rho(\mathbf{x}, t) \sum_{n=1}^{\infty} \frac{1}{n!} [(e^{\boldsymbol{\ell} \cdot \nabla_{\mathbf{x}}} - 1) \bar{\rho}(\mathbf{x}, t)]^n p(\boldsymbol{\ell})$$
$$= \int_{\mathbf{x},t} \left[\bar{\rho} \partial_t \rho + \frac{1}{\gamma} \partial_{\mathbf{x}} \bar{\rho} \cdot \int_{\mathbf{y}} \rho(\mathbf{x}, t) \partial_{\mathbf{x}} v(\mathbf{x} - \mathbf{y}) \rho(\mathbf{y}, t) \right] - \nu \int_{\mathbf{x},\boldsymbol{\ell},t} \rho(\mathbf{x}, t) \{\exp[(e^{\boldsymbol{\ell} \cdot \nabla_{\mathbf{x}}} - 1) \bar{\rho}(\mathbf{x}, t)] - 1\} p(\boldsymbol{\ell}). \tag{B10}$$

The linear order in the conjugated field gives back the Fokker-Planck equation, so the dynamic action can be expressed

$$S = \int_{\mathbf{x},t} (\bar{\rho} \partial_t \rho + \partial_{\mathbf{x}} \bar{\rho} \cdot \mathbf{D}_{\mathbf{x}} \rho) + \frac{1}{\gamma} \int_{\mathbf{x},\mathbf{y},t} (\rho \partial_{\mathbf{x}} \bar{\rho})(\mathbf{x}, t) \partial_{\mathbf{x}} v(\mathbf{x} - \mathbf{y}) \rho(\mathbf{y}, t) + \cdots, \tag{B11}$$

where we have used the representation of $\mathbf{D}_{\mathbf{x}}$ in term of the jump distribution in (9) and now the ellipsis denotes terms of higher order in $\bar{\rho}$. We introduce a new set of fields $\{a, \bar{a}\}$ related to the previous one $\{\rho, \bar{\rho}\}$ through the Cole-Hopf transformation as

$$\bar{a} = e^{\bar{\rho}}, \quad a = \rho e^{-\bar{\rho}}. \tag{B12}$$

Our aim is to show that the dynamic action can be simplified as

$$S = \int_{\mathbf{x},t} (\bar{a} \partial_t a + \partial_{\mathbf{x}} \bar{a} \cdot \mathbf{D}_{\mathbf{x}} a) + \frac{1}{\gamma} \int_{t,\mathbf{x},\mathbf{y}} (a \partial_{\mathbf{x}} \bar{a})(\mathbf{x}, t) \cdot \partial_{\mathbf{x}} v(\mathbf{x} - \mathbf{y})(a\bar{a})(\mathbf{y}, t)$$
$$= \int_{\mathbf{x},t} \left[\bar{a} \partial_t a + a \partial_{\mathbf{x}} \bar{a} \cdot \int_{\mathbf{y}} \partial_{\mathbf{x}} v(\mathbf{x} - \mathbf{y})(a\bar{a})(\mathbf{y}, t) \right] - \nu \int_{\mathbf{x},\boldsymbol{\ell},t} p(\boldsymbol{\ell}) [\bar{a}(\mathbf{x} + \boldsymbol{\ell}, t) - \bar{a}(\mathbf{x}, t)] a(\mathbf{x}, t), \tag{B13}$$

which is equivalent to demonstrating that

$$\int_{\mathbf{x}} e^{\bar{\rho}}(e^{-\boldsymbol{\ell}\cdot\nabla_{\mathbf{x}}}-1)(\rho e^{-\bar{\rho}}) = \int_{\mathbf{x}} \rho\{\exp[(e^{\boldsymbol{\ell}\cdot\nabla_{\mathbf{x}}}-1)\bar{\rho}]-1\}. \tag{B14}$$

The operator $e^{\boldsymbol{\ell}\cdot\nabla_{\mathbf{x}}}$ corresponds to the translation operator by a vector $\boldsymbol{\ell}$, whose effect on an arbitrary function $f(\mathbf{x})$ is given by

$$e^{\boldsymbol{\ell}\cdot\nabla_{\mathbf{x}}} f(\mathbf{x}) = f(\mathbf{x}+\boldsymbol{\ell}). \tag{B15}$$

Therefore, Eq. (B14) can be written as

$$\int_{\mathbf{x}} [\rho(\mathbf{x}-\boldsymbol{\ell})e^{\bar{\rho}(\mathbf{x})-\bar{\rho}(\mathbf{x}-\boldsymbol{\ell})}-\rho(\mathbf{x})] = \int_{\mathbf{x}} \rho(\mathbf{x})[e^{\bar{\rho}(\mathbf{x}+\boldsymbol{\ell})-\bar{\rho}(\mathbf{x})}-1]. \tag{B16}$$

Eventually, by translating the argument as $\mathbf{x}\to\mathbf{x}-\boldsymbol{\ell}$ in the first term on the right-hand side, the validity of this equation follows immediately.

[1] R. Kubo, Rep. Prog. Phys. **29**, 255 (1966).
[2] T. Vicsek, A. Czirók, E. Ben-Jacob, I. Cohen, and O. Shochet, Phys. Rev. Lett. **75**, 1226 (1995).
[3] J. Tailleur and M. E. Cates, Phys. Rev. Lett. **100**, 218103 (2008).
[4] V. Schaller, C. Weber, C. Semmrich, E. Frey, and A. R. Bausch, Nature (London) **467**, 73 (2010).
[5] Y. Fily and M. C. Marchetti, Phys. Rev. Lett. **108**, 235702 (2012).
[6] M. C. Marchetti, J. F. Joanny, S. Ramaswamy, T. B. Liverpool, J. Prost, M. Rao, and R. A. Simha, Rev. Mod. Phys. **85**, 1143 (2013).
[7] M. E. Cates and J. Tailleur, Annual Review of Condensed Matter Physics **6**, 219 (2015).
[8] A. Bricard, J.-B. Caussin, N. Desreumaux, O. Dauchot, and D. Bartolo, Nature (London) **503**, 95 (2013).
[9] H. H. Wensink, J. Dunkel, S. Heidenreich, K. Drescher, R. E. Goldstein, H. Löwen, and J. M. Yeomans, Proc. Natl. Acad. Sci. USA **109**, 14308 (2012).
[10] Y. Sumino, K. H. Nagai, Y. Shitaka, D. Tanaka, K. Yoshikawa, H. Chaté, and K. Oiwa, Nature (London) **483**, 448 (2012).
[11] J. Palacci, S. Sacanna, A. P. Steinberg, D. J. Pine, and P. M. Chaikin, Science **339**, 936 (2013).
[12] H. C. Berg, *E. coli in Motion* (Springer Science + Business Media, New York, 2008).
[13] M. J. Schnitzer, Phys. Rev. E **48**, 2553 (1993).
[14] J. Palacci, C. Cottin-Bizonne, C. Ybert, and L. Bocquet, Phys. Rev. Lett. **105**, 088304 (2010).
[15] I. Theurkauff, C. Cottin-Bizonne, J. Palacci, C. Ybert, and L. Bocquet, Phys. Rev. Lett. **108**, 268303 (2012).
[16] I. Buttinoni, J. Bialké, F. Kümmel, H. Löwen, C. Bechinger, and T. Speck, Phys. Rev. Lett. **110**, 238301 (2013).
[17] F. Ginot, I. Theurkauff, D. Levis, C. Ybert, L. Bocquet, L. Berthier, and C. Cottin-Bizonne, Phys. Rev. X **5**, 011004 (2015).
[18] P. Digregorio, D. Levis, A. Suma, L. F. Cugliandolo, G. Gonnella, and I. Pagonabarraga, Phys. Rev. Lett. **121**, 098003 (2018).
[19] T. F. F. Farage, P. Krinninger, and J. M. Brader, Phys. Rev. E **91**, 042310 (2015).
[20] G. Szamel, E. Flenner, and L. Berthier, Phys. Rev. E **91**, 062304 (2015).
[21] C. Maggi, U. Marini Bettolo Marconi, N. Gnan, and R. Di Leonardo, Sci. Rep. **5**, 10742 (2015).
[22] É. Fodor, C. Nardini, M. E. Cates, J. Tailleur, P. Visco, and F. van Wijland, Phys. Rev. Lett. **117**, 038103 (2016).
[23] R. Wittmann, C. Maggi, A. Sharma, A. Scacchi, J. M. Brader, and U. M. B. Marconi, J. Stat. Mech. (2017) 113207.
[24] R. Wittmann, U. M. B. Marconi, C. Maggi, and J. M. Brader, J. Stat. Mech. (2017) 113208.
[25] D. Mandal, K. Klymko, and M. R. DeWeese, Phys. Rev. Lett. **119**, 258001 (2017).
[26] D. Levis and L. Berthier, Phys. Rev. E **89**, 062301 (2014).
[27] U. Seifert, Rep. Prog. Phys. **75**, 126001 (2012).
[28] L. Berthier and J. Kurchan, Nat. Phys. **9**, 310 (2013).
[29] E. Ben-Isaac, Y. K. Park, G. Popescu, F. L. H. Brown, N. S. Gov, and Y. Shokef, Phys. Rev. Lett. **106**, 238103 (2011).
[30] É. Fodor, M. Guo, N. S. Gov, P. Visco, D. A. Weitz, and F. van Wijland, Europhys. Lett. **110**, 48005 (2015).
[31] É. Fodor, W. W. Ahmed, M. Almonacid, M. Bussonnier, N. S. Gov, M.-H. Verlhac, T. Betz, P. Visco, and F. van Wijland, Europhys. Lett. **116**, 30008 (2016).
[32] J. Roberts, J. Sound Vib. **24**, 23 (1972).
[33] M. Grigoriu, J. Eng. Mech. **113**, 757 (1987).
[34] M. Di Paola and G. Falsone, *Nonlinear Stochastic Mechanics: IUTAM Symposium, Turin, 1991* (Springer, Berlin, 1992), pp. 155–166.
[35] M. Di Paola and G. Falsone, J. Appl. Mech. **60**, 141 (1993).
[36] M. D. Paola and G. Falsone, Prob. Eng. Mech. **8**, 197 (1993).
[37] M. Grigoriu, Prob. Eng. Mech. **10**, 171 (1995).
[38] A. Pirrotta, Prob. Eng. Mech. **22**, 127 (2007).
[39] D. M. Popescu and O. Lipan, PLoS One **10**, e0116752 (2015).
[40] K. Kanazawa, T. Sueshige, H. Takayasu, and M. Takayasu, Phys. Rev. Lett. **120**, 138301 (2018).
[41] M. O. Cáceres and A. A. Budini, J. Phys. A: Math. Gen. **30**, 8427 (1997).
[42] A. Dubkov and B. Spagnolo, Fluct. Noise Lett. **5**, L267 (2005).
[43] W. A. M. Morgado, S. M. D. Queirós, and D. O. Soares-Pinto, J. Stat. Mech. (2011) P06010.
[44] W. A. M. Morgado and S. M. D. Queirós, Phys. Rev. E **93**, 012121 (2016).
[45] K. Kanazawa, T. Sagawa, and H. Hayakawa, Phys. Rev. Lett. **108**, 210601 (2012).
[46] K. Kanazawa, T. G. Sano, T. Sagawa, and H. Hayakawa, Phys. Rev. Lett. **114**, 090601 (2015).
[47] K. Kanazawa, T. G. Sano, T. Sagawa, and H. Hayakawa, J. Stat. Phys. **160**, 1294 (2015).
[48] T. G. Sano, K. Kanazawa, and H. Hayakawa, Phys. Rev. E **94**, 032910 (2016).

[49] K. Kanazawa, *Statistical Mechanics for Athermal Fluctuation: Non-Gaussian Noise in Physics* (Springer, Berlin, 2017).
[50] M. E. Cates and J. Tailleur, Europhys. Lett. **101**, 20010 (2013).
[51] G. S. Redner, M. F. Hagan, and A. Baskaran, Phys. Rev. Lett. **110**, 055701 (2013).
[52] D. S. Dean, J. Phys. A: Math. Gen. **29**, L613 (1996).
[53] K. Kawasaki, Physica A **208**, 35 (1994).
[54] J.-P. Hansen and I. R. McDonald, *Theory of Simple Liquids*, 4th ed. (Academic, Oxford, 2013).
[55] N. G. van Kampen, *Stochastic Processes in Physics and Chemistry*, 2nd ed. (North-Holland, Amsterdam, 1992).
[56] H. Risken, *The Fokker-Planck Equation: Methods of Solutions and Applications*, 2nd ed. (Springer, Berlin, 1996).
[57] C. Gardiner, *Handbook of Stochastic Methods: for Physics, Chemistry and the Natural Sciences*, 3rd ed. (Springer, Berlin, 2004).
[58] A. P. Solon, M. E. Cates, and J. Tailleur, Eur. Phys. J. Spec. Top. **224**, 1231 (2015).
[59] G. Szamel, Phys. Rev. E **90**, 012111 (2014).
[60] É. Fodor, H. Hayakawa, P. Visco, and F. van Wijland, Phys. Rev. E **94**, 012610 (2016).
[61] J. Elgeti and G. Gompper, Europhys. Lett. **85**, 38002 (2009).
[62] J. Tailleur and M. Cates, Europhys. Lett. **86**, 60002 (2009).
[63] S. Das, G. Gompper, and R. G. Winkler, New J. Phys. **20**, 015001 (2018).
[64] M. B. Miller and B. L. Bassler, Annu. Rev. Microbiol. **55**, 165 (2001).
[65] C. Liu, X. Fu, L. Liu, X. Ren, C. K. Chau, S. Li, L. Xiang, H. Zeng, G. Chen, L.-H. Tang, P. Lenz, X. Cui, W. Huang, T. Hwa, and J.-D. Huang, Science **334**, 238 (2011).
[66] J. Bialké, H. Löwen, and T. Speck, Europhys. Lett. **103**, 30008 (2013).
[67] A. G. Thompson, J. Tailleur, M. E. Cates, and R. A. Blythe, J. Stat. Mech. (2011) P02029.
[68] R. Soto and R. Golestanian, Phys. Rev. E **89**, 012706 (2014).
[69] A. B. Slowman, M. R. Evans, and R. A. Blythe, Phys. Rev. Lett. **116**, 218101 (2016).
[70] A. P. Solon, Y. Fily, A. Baskaran, M. E. Cates, Y. Kafri, M. Kardar, and J. Tailleur, Nat. Phys. **11**, 673 (2015).
[71] A. P. Solon, J. Stenhammar, M. E. Cates, Y. Kafri, and J. Tailleur, New J. Phys. **20**, 075001 (2018).
[72] J. D. Weeks, D. Chandler, and H. C. Andersen, J. Chem. Phys. **54**, 5237 (1971).
[73] A. Velenich, C. Chamon, L. F. Cugliandolo, and D. Kreimer, J. Phys. A: Math. Theor. **41**, 235002 (2008).
[74] M. Doi, J. Phys. A: Math. Gen. **9**, 1465 (1976).
[75] L. Peliti, J. Phys. (Paris) **46**, 1469 (1985).
[76] P. Grassberger, Z. Phys. B **47**, 365 (1982).
[77] J. Yvon, *La Théorie Statistique des Fluides et l'Équation d'État* (Hermann & Cie, Paris, 1935), Vol. 203.
[78] M. Born and H. S. Green, Proc. R. Soc. Med. **188**, 10 (1946).
[79] C. Bechinger, R. Di Leonardo, H. Löwen, C. Reichhardt, G. Volpe, and G. Volpe, Rev. Mod. Phys. **88**, 045006 (2016).
[80] É. Fodor and M. C. Marchetti, Physica A **504**, 106 (2018).
[81] K. Martens, L. Angelani, R. Di Leonardo, and L. Bocquet, Eur. Phys. J. E **35**, 84 (2012).
[82] L. Angelani, A. Costanzo, and R. D. Leonardo, Europhys. Lett. **96**, 68002 (2011).
[83] N. Koumakis, C. Maggi, and R. Di Leonardo, Soft Matter **10**, 5695 (2014).
[84] C. Sandford, A. Y. Grosberg, and J.-F. Joanny, Phys. Rev. E **96**, 052605 (2017).
[85] C. J. O. Reichhardt and C. Reichhardt, Annual Review of Condensed Matter Physics **8**, 51 (2017).
[86] K. Kanazawa, T. Sagawa, and H. Hayakawa, Phys. Rev. E **90**, 012115 (2014).
[87] R. Zakine, A. Solon, T. Gingrich, and F. van Wijland, Entropy **19**, 193 (2017).
[88] D. Chaudhuri, A. Raju, and A. Dhar, Phys. Rev. E **91**, 050103 (2015).
[89] D. Martin, C. Nardini, M. E. Cates, and É. Fodor, Europhys. Lett. **121**, 60005 (2018).